Feline Congenital Erythropoietic Porphyria: Two Homozygous *UROS* Missense Mutations Cause the Enzyme Deficiency and Porphyrin Accumulation

Sonia Clavero,[1] David F Bishop,[1] Urs Giger,[2] Mark E Haskins,[2] and Robert J Desnick[1]

[1]Department of Genetics and Genomic Sciences, Mount Sinai School of Medicine, New York, New York, United States of America; [2]Section of Medical Genetics, School of Veterinary Medicine, University of Pennsylvania, Philadelphia, Pennsylvania, United States of America

The first feline model of human congenital erythropoietic porphyria (CEP) due to deficient uroporphyrinogen III synthase (URO-synthase) activity was identified by its characteristic clinical phenotype, and confirmed by biochemical and molecular genetic studies. The proband, an adult domestic shorthair cat, had dark-red urine and brownish discolored teeth with red fluorescence under ultraviolet light. Biochemical studies demonstrated markedly increased uroporphyrinogen I in urine and plasma (2,650- and 10,700-fold greater than wild type, respectively), whereas urinary 5-aminolevulinic acid and porphobilinogen were lower than normal. Erythrocytic URO-synthase activity was <1% of mean wild-type activity, confirming the diagnosis and distinguishing it from feline phenocopies having acute intermittent porphyria. Sequencing of the affected cat's *UROS* gene revealed two missense mutations, c.140C>T (p.S47F) in exon 3 and c.331G>A (p.G111S) in exon 6, both of which were homozygous, presumably owing to parental consanguinity. Neither was present in 100 normal cat alleles. Prokaryotic expression and thermostability studies of the purified monomeric wild-type, p.S47F, p.G111S, and p.S47F/G111S enzymes showed that the p.S47F enzyme had 100% of wild-type specific activity but ~50% decreased thermostability, whereas the p.G111S and p.S47F/G111S enzymes had about 60% and 20% of wild-type specific activity, respectively, and both were markedly thermolabile. Molecular modeling results indicated that the less active/less stable p.G111S enzyme was further functionally impaired by a structural interaction induced by the presence of the S47F substitution. Thus, the synergistic interaction of two rare amino acid substitutions in the URO-synthase polypeptide caused the feline model of human CEP.

INTRODUCTION

Congenital erythropoietic porphyria (CEP) is an autosomal recessive inborn error of heme biosynthesis resulting from the markedly deficient, but not absent, activity of uroporphyrinogen III synthase (URO-synthase, EC 4.2.1.75), a characteristic that distinguishes this disorder from feline phenocopies having acute intermittent porphyria (AIP) (1,2). The URO-synthase enzyme converts the linear tetrapyrrole hydroxymethylbilane (HMB) to uroporphyrinogen (URO'gen) III.

When URO-synthase activity is deficient, the accumulated HMB is nonenzymatically converted to the URO'gen I isomer, which can be enzymatically converted to the metabolic end product, coproporphyrinogen (COPRO'gen) I. The accumulated URO'gen I and COPRO'gen I isomers are oxidized to their corresponding porphyrins, uroporphyrin I (URO I) and coproporphyrin I (COPRO I).

The severity of human CEP ranges from hydrops fetalis *in utero* to a later-onset phenotype characterized only by mild cutaneous involvement (2–4). Clinical severity depends primarily on the amount of residual URO-synthase activity, and phenotype/genotype correlations have been reported (for example, [5,6]). In CEP, URO I and COPRO I isomers accumulate in erythroid precursors and erythrocytes, which can rupture and release these porphyrins into the circulation, leading to their deposition in skin, tissues and bones, and excretion in the urine and feces. When the photocatalytic URO I and COPRO I in the skin are exposed to sunlight, a free-radical reaction results in blistering, vesicle formation and scarring. Secondary infection of the cutaneous lesions can lead to disfigurement of the face and hands (2–4). Porphyrin deposition in the teeth and bones causes the clinically diagnostic reddish-brown discolored teeth (i.e., erythrodon-

---

Address correspondence and reprint requests to Robert J Desnick, Department of Genetics and Genomic Sciences, Mount Sinai School of Medicine, Fifth Avenue at 100th Street, New York, NY 10029-6574. Phone: 212-659-6700; Fax: 212-360-1809; E-mail: robert.desnick@mssm.edu.

tia). Medical management is focused on protecting affected individuals from sun or ultraviolet (UV)-light exposure and maintaining adequate hematopoesis. Patients with severe hemolysis have chronic transfusion-dependent anemia and may develop splenomegaly. Therapeutic efforts have included hematopoietic stem cell transplantation (7–10), and efforts are underway to develop hematopoietic gene transfer to continuously replace the defective gene (11–13).

The human and murine URO-synthase cDNA and genomic sequences have been isolated and characterized (14,15). In both species, the URO-synthase gene has 10 exons and 2 mRNA transcripts generated by alternative splicing, directed from unique housekeeping and erythroid-specific promoters. The housekeeping mRNA is generated by splicing together exons 1, 2B and 3 through 10, whereas the erythroid-specific mRNA contains exons 2A, 2B and 3 through 10 (14). Both the housekeeping and erythroid-specific mRNAs express the same URO-synthase amino acid sequence, because the initiation ATG codon is in exon 2B, shared by both the housekeeping and erythroid transcripts. The wild-type human enzyme is a monomer of 265 residues and functions in the cytosol. Recently, the three-dimensional structure of the human enzyme was determined (16–18), and the initial feline *UROS* genomic sequence was reported (19). However, the housekeeping and erythroid-specific exons were not identified, nor was the exon structure confirmed by sequence analysis of the feline URO-synthase cDNAs.

Naturally occurring animal models of congenital porphyria with erythrodontia were described decades ago in cattle (20–22), pigs (21,23) and cats (24,25). A previously reported feline model had an autosomal dominant CEP-like phenotype (that is, erythrodontia) and elevated urinary and/or tissue PBG, URO and COPRO. Recently, we have shown that cats with autosomal dominant erythrodontia actually had AIP (1). Now, we report the first naturally-occurring feline

model of CEP based on enzyme, porphyrin and molecular genetic studies.

MATERIALS AND METHODS

Proband

The proband was a neutered 10-year-old male domestic shorthair cat who was referred from Amherst, Wisconsin, because the cat had brownish discolored teeth. When examined, his teeth fluoresced pink (Figure 1), but no other clinical signs were noted. No family history was available, because the proband was adopted at 9 years of age. Complete blood cell counts and blood cell morphology were normal except for a mild normoblastosis, basophilic stipling and polychromasia. Blood lead levels were negative, and all other routine laboratory analyses were within normal limits. Fresh blood and urine samples were obtained from the proband and healthy adult cats. Animal procedures were approved by the University of Pennsylvania Institutional Animal Care and Use Committee.

Biochemical Studies

Fresh frozen erythrocytes (3–5 mL) from the proband and healthy wild-type cats were lysed in 3 volumes of 50 mmol/L K-Hepes, pH 7.5, 0.02% sodium azide, 0.1% Triton X-100, and 1 mmol/L dithiothreitol and centrifuged at $10,000g$ for 10 min. URO-synthase and hydroxymethylbilane synthase (HMB-synthase) activities were measured in the cleared erythrocyte lysates from the proband and wild-type cats as previously described (26,27). For porphyrin analyses, urine, plasma and erythrocyte lysates were deproteinized by addition of 20% trichloroacetic acid in dimethyl sulfoxide/lysate 1:1 (v/v) followed by centrifugation at $10,000g$ for 10 min. Porphyrin isomers in deproteinized samples were resolved and quantitated by ultraperformance liquid chromatography with fluorescence monitoring as previously described (1). The levels of the porphyrin precursors, aminolevulinic acid (ALA) and porphobilinogen (PBG),

were determined in urine from the proband and wild-type adult cats by using the ALA/PBG Column Test kit (Bio-Rad Laboratories, Hercules, CA, USA) according to the manufacturer's instructions.

Molecular Analyses

Genomic DNA was isolated from whole blood obtained from the proband and wild-type cats by using the Puregene® Genomic DNA Purification kit (Gentra Systems, Minneapolis, MN, USA). The feline *UROS* gene was amplified from genomic DNA by using the HotStarTaq® MasterMix (Qiagen, Valencia, CA, USA) by the polymerase chain reaction (PCR) with the primers and annealing temperatures listed in Supplemental Table 1. Briefly, PCR amplification was performed by using the following sequential steps: 95°C for 15 min, then 31 cycles of amplication with denaturation at 95°C for 30 s, extension at the annealing temperature (Supplemental Table 1) for 30 s, a 1°C/s ramp to 72°C, followed by 72°C for 30 s, and then a final extension at 72°C for 10 min.

RNA was extracted, purified and retrotranscribed in one step from liver and spleen as previously described (1). The primers for each cDNA region are listed in Supplemental Table 1B. The cDNA and genomic sequences and electropherogram traces were compared by using the CodonCode Aligner (CodoCode Corp., Dedham, MA, USA). The individual amplicons were sequenced by using the amplification primers on an Applied Biosystems Model 3730xl DNA Analyzer (Foster City, CA, USA).

Because the cat *UROS* genomic sequences (GenBank accession numbers ACBE01376257 and ACBE01376259) lacked identification of the housekeeping and erythroid-specific exons and promoters, and because the predicted intron/exon boundaries had been assigned by homology to those in other organisms, the feline genomic organization and sequence were determined by sequencing

the *UROS* gene in the domestic shorthair cat by using primer selection based on homology with the human *UROS* gene structure. For delineation of the feline gene's intron-exon boundaries, the sequences of reverse-transcribed feline erythroid and housekeeping *UROS* mRNAs were determined and compared with the exon-flanking intronic regions by using ClustalW (MacVector; MacVector Inc., Cary, NC, USA).

To determine if the two missense mutations detected in the proband's URO-synthase sequence were polymorphisms, we evaluated their presence in 100 normal alleles from domestic shorthair cats. For the exon 3 c.140C>T (p.S47F) mutation, a region of 153 bp was amplified with primers FmU-S47F-F and FmU-S47F-R (Supplemental Table 1), and the amplicon was digested with the restriction enzyme *Dde*I (New England Biolabs, Ipswich, MA, USA). The c.140C>T mutation obliterated the *Dde*I restriction site at position 119 of the amplified region, resulting in a single 153-bp band for the proband, whereas the wild-type amplicons had 119- and 34-bp bands visualized by agarose gel electrophoresis and staining with ethidium bromide. For the c.331G>A (p.G111S) mutation, a region of 150 bp was amplified with primers FmU-G111S-F and FmU-G111S-R (Supplemental Table 1) and digested with *Hae*III (New England Biolabs). Absence of the mutation yielded *Hae*III fragments of 100 and 50 bp, whereas the 150 bp amplicon was not digested when the mutation was present (Supplemental Table 1).

Prokaryotic Expression of the Recombinant Feline URO-Synthase Missense Mutations

The full-length feline URO-synthase coding cDNA was amplified (see primers in Supplemental Table 1) and subcloned into the pSU vector as described (1), and the c.140C>T and c.331G>A mutations were individually or sequentially introduced into the cDNA using the QuikChange® II Site-Directed Mutagenesis kit (Stratagene,

La Jolla, CA, USA), according to the manufacturer's instructions. *Escherichia coli* BL21 Codon Plus® transformants were grown in SuperBroth medium (MP Biomedicals LLC, Solon, OH, USA), expression was induced for 4 h with 1 mmol/L IPTG and the cells were harvested by centrifugation at 5,000g for 20 min after reaching an absorbance of ~2.0 at 600 nm. The cell pellets were resuspended in 50 mmol/L HEPES pH 7.8, 0.5 mol/L NaCl, 5 mg/mL DNAse, 5 mg/mL RNAse, 5 mmol/L tris[2-carboxyethyl] phosphine (TCEP; Fisher Scientific, Pittsburgh, PA, USA), 330 mg/mL lysozyme, and 1 μmol/L leupeptin and then lysed by three cycles of freeze/thaw in ethanol/dry ice and a 37°C water bath and then centrifuged at 10,000g for 30 min. The expressed feline enzyme was purified by two consecutive affinity chromatographic steps on nickel-agarose resin (IMAC Sepharose High Performance; GE Healthcare, Piscataway, NJ, USA). The eluate was concentrated and the buffer exchanged to 50 mmol/L HEPES, pH 7.4, 100 mmol/L NaCl and 5 mmol/L TCEP by using an Amicon Ultra-15 Centrifugal Filter Unit, 10-kDa cutoff (Millipore, Billerica, MA, USA). URO-synthase activity was measured as described previously (27). One unit of activity is the amount of enzyme that produces 1 nmol of uroporphyrin III in 1 h under the conditions of the assay.

Thermostability Studies

Following expression of the mutant and wild-type constructs as described above, purified enzyme preparations were adjusted to 50 mmol/L HEPES, pH 7.4, 100 mmol/L NaCl and 5 mmol/L dithiothreitol, and aliquots were incubated at 50°C for up to 1 h. Aliquots were removed to ice at regular intervals and URO-synthase activity was determined.

Structural Studies

The three-dimensional structures of the feline wild-type and mutant URO-synthase enzymes were generated by

using the SWISS-MODEL server (swissmodel.expasy.org; Swiss Institute of Bioinformatics, Lausanne, Switzerland) (28). Four separate feline URO-synthase structures were modeled for the wild-type, p.S47F, p.G111S and doubly mutant p.S47F/G111S enzymes by using the crystal structure of human URO-synthase (PDB entry 1JR2A) as the template. The alignment mode was used, based on a MacVector ClustalW alignment of 19 vertebrate URO-synthase sequences (GenBank accession numbers: NP_000366, XP_508102, XP_001086303, XP_001925339, XP_001490208, EFB30103, XP_854192, XP_001790343, NP_001012068, NP_033505, XP_001362178, XP_423886, XP_002193805, NP_001087355, NP_001107324, ACO13405, ACM08595 and NP_997993) and the feline sequence from this study. The modeled structures were visualized with the PyMOL Molecular Graphics System, Version MacPyMOL98, (Schrödinger, New York, NY, USA). The MacPyMOL Measurement Wizard was used to obtain atomic distances between altered positions of residue atoms for pairwise comparisons between the wild-type and mutant structures.

Web Deposition of Data

The housekeeping cDNA, erythroid cDNA and genomic exons 1, 2 and 3 with flanking sequences were deposited in GenBank (http://www.ncbi.nlm.nih.gov/gene/) as HQ159393, HQ159394, and HQ159395, respectively.

All supplementary materials are available online at www.molmed.org.

RESULTS

Biochemical Studies

Urinary ALA and PBG concentrations were not increased in the proband, whereas the levels of URO I and COPRO I were markedly elevated, to ~2,600- and ~245-fold greater than the respective mean wild-type values (Table 1). The plasma levels of URO I and COPRO I also were markedly in-

Table 1. Urinary porphyrin precursors and porphyrins in the affected proband and wild-type (WT) cats.

Precursor/porphyrin	WT (n = 8), μmol/mol Cr (range)[a]	Wisconsin (r = 3)[b]		
		μmol/mol Cr (range)	Fold change over WT	Percent of total I + III isomers
ALA	2,400 (980–4,300)	1100 (816–1,370)	0.46	NA[c]
PBG	650 (200–2,200)	150 (60–210)	0.23	NA[c]
URO I	0.40 (0.23–0.62)	1060 (480–1,480)	2,650	69.3
URO III	0.20 (0.10–0.35)	38 (20–58)	190	2.5
URO I/III ratio	2.0	28	14	
COPRO I	1.7 (1.4–1.9)	416 (190–566)	245	27.2
COPRO III	0.72 (0.48–0.90)	15 (7–19)	20	1.0
COPRO I/III ratio	2.4	28	12	

[a]Normal values are as previously published (1).
[b]n = 1, r = 3 denotes three replicate assays.
[c]NA, not applicable.

Table 2. Erythrocyte and plasma porphyrins in the affected proband and WT cats.

Tissue and porphyrin	WT (n = 6), nmol/L tissue[a] (range)	Wisconsin (n = 1)		
		nmol/L Tissue (range)	Fold over WT	Percent of total I + III isomers
Erythrocytes				
URO I	0.61 (0.0–1.22)	113	185	41.5
URO III	0.1 (0–0.1)	2.51	25.1	0.9
COPRO I	0.07 (0–0.14)	155	2,210	57.5
COPRO III	0.1 (0–0.1)	ND[b]	ND[b]	0.0
PROTO IX	ND[b]	ND[b]	ND[b]	ND[b]
Plasma				
URO I	0.12 (0–0.17)	1,283 (1,123–1,443)	10,700	45.6
URO III	0.10 (0–0.39)	ND[b]	ND[b]	0.0
COPRO I	0.29 (0.15–0.53)	1,530 (1,376–1,684)	5,280	54.4
COPRO III	0.18 (0.11–0.28)	ND[b]	ND[b]	0.0

[a]Normal values of porphyrins in a liter of packed erythrocytes are as previously published (1).
[b]ND, not detectable. The limit of detection of porphyrins was 0.1 pmol/g tissue.

creased over respective wild-type mean levels, ~11,000- and ~5,300-fold, respectively (Table 2). In erythrocytes, URO I and COPRO I were elevated ~180- and ~2,200-fold, respectively (Table 2). Protoporphyrin IX was not elevated in urine or blood. As shown in Table 3, the URO-synthase enzymatic activity in erythrocytes from the proband was less than 1% of the mean wild-type feline activity, whereas the HMB-synthase levels were increased several fold, confirming the clinical and biochemical diagnosis of CEP.

Molecular Analyses

The exon/intron structure of the feline gene was found to be identical to that of the previously reported mouse and human URO-synthase genes (14,15), and the 5′UTRs of each transcript and approximate location of the housekeeping and erythroid promoters were identified (Supplemental Table 2). Because the 5′-ends of the housekeeping exon 1 and the ery-

throid-specific exon 2A were sequenced by using exonic primers, the transcription start sites in the cat were not determined. Of note, the full-length UROS polypeptide was one amino acid shorter than in primates and rodents, ending (as in canines) in one cysteine instead of two.

Table 3. Enzyme activities in erythrocytes of the affected proband and WT cats.

Enzyme	WT, U/mg protein, (n)[a] (range)	Wisconsin (n = 1)	
		U/mg protein (n)[a]	% of WT
HMB-synthase	0.017 (3) (0.015–0.021)	0.056 (1)	330
URO-synthase	0.54 (1) (0.43–0.62)[b]	0.0036 (2)	0.67

[a]Expressed purified WT activity: 1 U = nmol product/h/mg protein.
[b]Range for 5 replicates.

Table 4. Prokaryotic expression and characterization of the purified wild-type and mutant URO-synthase enzymes of the CEP cat.

| cDNA mutation | Predicted protein | Specific activity, % of WT (n)[a] | Total purified expressed enzyme protein,[b] % of WT | Thermolability at 50°C[c] | |
				$T_{1/2}$ (n) (min)[d]	% of Initial at 15 min, %[e]
WT	None	100 (8)	100	9.0 (4)	28
c.140C>T	p.S47F	100 (5)	59	4.8 (2)	11
c.331G>A	p.G111S	59 (4)	10	1.3 (2)	0.1
c.140C>T/c.331G>A	p.S47F/p.G111S	19 (7)	2	1.6 (2)	0.3

[a]100% = 571,000 nmoles/h/mg protein.
[b]100% = 35.3 mg/L of expression culture; n = 1.
[c]50°C, pH, 7.4.
[d]The results at time = 15 min were calculated from the linear semilog plots from which the $T_{1/2}$ values were determined.
[e]Percent of initial enzyme activity.

For feline HMB-synthase, sequence analysis of the entire coding region and flanking intronic sequences of the proband and wild-type feline genes revealed normal sequences with no exonic polymorphisms compared with the recently deposited hepatic and erythroid feline sequences (GenBank Accession numbers CQ850461-4) (1).

URO-Synthase Mutation Detection and Expression

Sequencing of the proband's URO-synthase gene revealed two homozygous missense mutations: a C-to-T transition at position 140 in exon 3 (c.140C>T) predicting the substitution of a phenylalanine for a serine residue (p.S47F) and a G-to-A transition at position 331 in exon 6 (c.331G>A) predicting the replacement of a glycine by a serine residue (p.G111S). Analysis of 100 feline wild-type alleles for the c.140C>T and c.331G>A mutations did not detect these changes, suggesting that they were not common polymorphisms.

Each mutation was introduced separately and together into the feline URO-synthase full-length cDNA and expressed in *E. coli*. The purified feline p.S47F enzyme had normal activity, whereas the feline p.G111S enzyme had ~60% of expressed wild-type activity (Table 4). When the cDNA construct with both mutations was expressed, the purified doubly mutant (p.S47F/G111S) enzyme's activity was markedly reduced to ~20% of expressed wild-type activity. However, the yield of purified enzyme

was only ~2% of the purified expressed wild-type enzyme (Table 4). When incubated at 50°C at pH 7.4 for 15 min, the wild-type enzyme retained 28% of initial activity, whereas the p.S47F, p.G111S and doubly mutant p.S47F/G111S enzymes had 11%, 0.1% and 0.3% of their initial activities, respectively (Table 4).

Molecular Modeling of the Feline Wild-Type and Mutant Enzymes

The three-dimensional structures of the wild-type and three mutant feline URO-synthase enzymes (p.S47F, p.G111S and p.S47F/G111S), were modeled as described in Materials and Methods. The total energies calculated for the wild-type, p.S47F, p.G111S and p.S47F/G111S structure models were 8,802, 8,790, 7,512 and 6,950 kJ/mol, respectively, consistent with the observed decreased relative stability of the p.G111S and doubly mutant proteins. Three distinct clusters of three amino acids each exhibited positional differences compared with the wild-type feline structure. Cluster 1 was located in the previously identified active site (16,18,29) in the cleft between domains 1 and 2 and contained residues Asp8, Leu36 and Lys170. Cluster 2 was located in domain 1 directly above the hinge β sheet and contained residues Ser47 or Phe47, Asp77 and Lys79. Cluster 3 contained residues Lys88, Ile110 and G111 or S111, and was located in domain 1 between two α helices whose connecting vertex contained the Asp77 and Lys79 of cluster 2. For cluster 1, the movements of the three residues' backbone and side-

chain atoms (not including hydrogens) were modest, being greatest between the wild-type and the p.S47F/G111S structures (totaling 2.76 Å; data not shown) and were essentially uninfluenced by the presence of the p.G111S mutation alone. Larger atomic movements were noted in cluster 2 (totaling 15.71 Å) and were greatest between residue atoms for the p.S47F structure compared with the p.G111S structure (data not shown). As in cluster 1, the cause of the movements could be attributed almost completely to the substitution of the bulky Phe47 substitution. In contrast, for cluster 3, a unique interaction with cluster 2 was observed. This interaction was most notable for residue 111, where the positions of the Ser111 backbone atoms in the double-mutant structure (Figure 2C) were intermediately between their positions in the p.S47F (Figure 2A) and p.G111S mutant structures (Figure 2B). The greatest total atomic movement in cluster 3 (4.86 Å; data not shown) was between the p.S47F and p.G111S structures. Some movement was also seen for residue Leu112 near this cluster (data not shown).

DISCUSSION

Previously, cats who presented with brownish discolored teeth that fluoresced pink under UV light and had increased URO and COPRO concentrations were reported as having a "congenital porphyria" or CEP (24,25,30,31). However, the feline disease was inherited as an autosomal
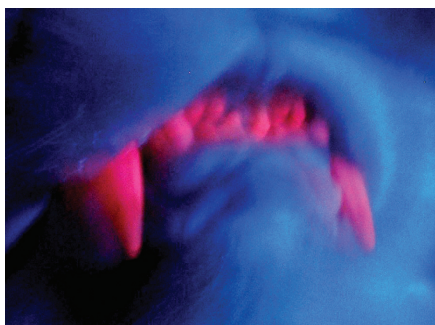
Figure 1. Photograph of the proband's teeth under UV light. No filter was used, so the blue color is the reflected light from the blue UV lamp bulb.

dominant trait, as it was in some pig models (21,23,32,33), whereas in humans and cattle the disease is inherited only as an autosomal recessive trait (2,22,32,34). Recently, this conundrum was clarified, because cats with the CEP-like phenotype and autosomal dominant inheritance were shown to actually have AIP (1). The AIP cats had elevated urinary ALA and PBG levels, half-normal activities of HMB-synthase

activity in erythrocytes and tissues and normal or slightly elevated erythrocyte URO-synthase activities (1).

During evaluation of additional referred cats with the CEP-like phenotype, the proband reported here was identified. In urine, he had markedly elevated URO I and COPRO I, but normal levels of ALA and PBG, and normal erythrocyte HMB-synthase activity (Tables 1–3). Although expressing urinary URO III and COPRO III as fold increases over wild type gives the impression of large (25–200)-fold increases, it should be noted that wild-type levels are very low, and the 200-fold increase resulted in only 3.4% III isomer compared with the total—the vast majority being the I isomer (Table 1). Thus the III-isomer elevation was not a significant contributor to the porphyria. Even less III isomer was observed in erythrocytes and plasma; 0.9% and 0.0%, respectively (Table 2). These results contrast with much higher percentages (65% and 31% in erythrocytes and urine) for the AIP cats. In the proband,

erythrocyte URO-synthase activity was nearly absent, consistent with the diagnosis of CEP (Table 3). The clinical and biochemical features of the AIP and CEP cats are summarized in Table 5.

Surprisingly, the CEP proband was homozygous for two missense mutations in the URO-synthase gene, c.140C>T (p.S47F) and c.331G>A (p.G111S). Neither of these lesions was a common feline polymorphism, based on screening results of 100 wild-type domestic shorthair alleles. Presumably, both lesions occurred independently, because the simultaneous occurrence of two point mutations in different exons is unlikely. Possibly, the c.140C>T mutation arose first, because it does not significantly alter enzyme activity. This mutation may have occurred in the community of domestic shorthair cats in Wisconsin. The c.331G>A mutation occurred at a CpG dinucleotide, a known hotspot of mutation (35). The presence of two mutations in the feline *UROS* gene, both homozygous, presumably resulted from parental cosanguinity, because the proband was
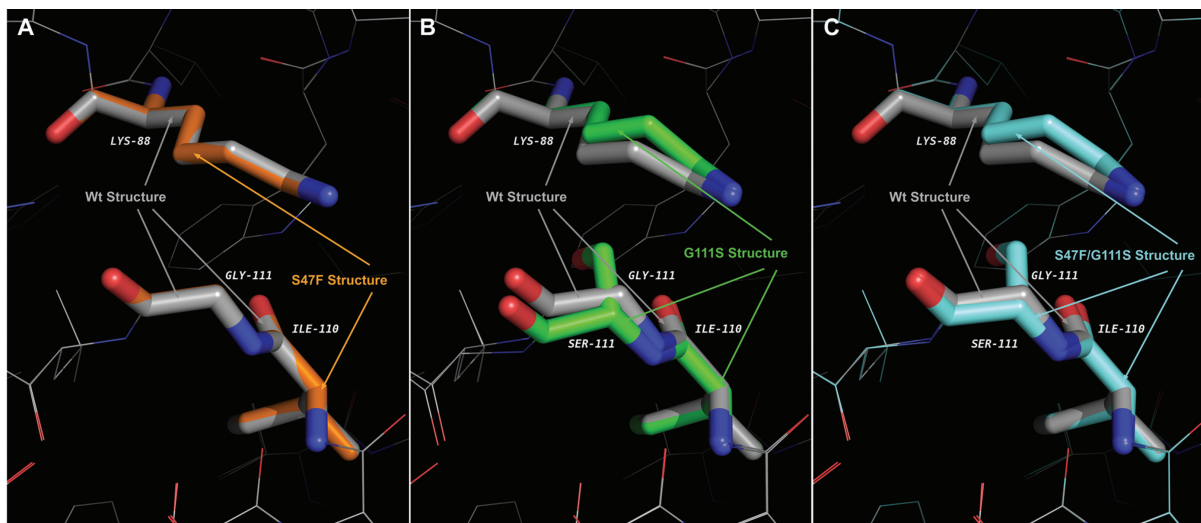
Figure 2. Effect of the individual and combined CEP mutations on the predicted three-dimensional structures of feline URO synthase. Each of the three panels are overlays of the wild-type structure and one of the mutant structures in the region of cluster 2, containing amino acids Lys 88, Ile 110 and Gly 111. (A) Comparison of the wild-type structure (residues colored in gray) with the S47F structure (residues colored in orange). (B) Comparison of the wild-type structure with the G111S structure (residues colored in green). (C) Comparison of the wild-type structure with the S47F/G111S structure (residues colored in blue). Note particularly that the position of Serine 111 in the structure of the combined S47F/G111S mutation structure is intermediate in position between that of the wild-type Glycine 111 and the Serine 111 of the G111S structure.

Table 5. Characteristics of feline AIP and CEP

Feature	Feline AIP	Feline CEP
Brownish teeth (erythodontia) that fluoresce	+	+
Inheritance	Autosomal dominant	Autosomal recessive
HMB-synthase activity	Half-normal	Normal
URO-synthase activity	Normal or increased	<1%
Urinary ALA	Normal or slightly increased	Normal
Urinary PBG	Increased 3–13-fold	Normal
Urinary URO I	Increased 240-fold	Increased 2,700-fold
Urinary URO III	Increased 220-fold	Increased 190-fold
Erythrocyte III isomer,[a] %	65%	0.9%
Urine III isomer, %	31%	3.4%

[a]100 × (URO III + COPRO III)/(URO I + URO III + COPRO I + COPRO III).

homozygous for 25 intronic polymorphic sites in the URO-synthase gene compared with 16 of 25 for a wild-type cat.

Mutagenesis and expression studies of the feline URO-synthase mutant constructs indicated that the purified p.S47F enzyme had normal specific activity and modest thermolability, whereas the purified p.G111S mutant enzyme had ~60% of wild-type activity and was markedly more thermolabile (Table 4). Notably, expression of the disease-causing allele having both the c.140C>T and c.331G>A mutations resulted in an enzyme protein (p.S47F/G111S) that had markedly reduced activity compared with the p.G111S enzyme, but similar thermolability (Table 4). Of particular note, the yield of the purified expressed p.S47F/G111S active enzyme was ~2% of wild type, suggesting that the doubly mutant enzyme did not fold properly and/or was susceptible to intracellular degradation.

Modeling studies comparing the predicted wild-type and mutant enzyme structures were informative because the feline and human enzymes had 86% amino acid identity. Although the p.S47F substitution generated the greatest motion in the three affected residue clusters, it alone had no effect on the mutant enzyme's activity but reduced its thermostability by ~50%. In contrast, the p.G111S substitution had a major effect on both the activity and thermostability of the p.G111S enzyme. Glycine is known to contribute to turn formation in protein

structures and indeed, G111 is located at the apex of a turn between two helicies in the enzyme. Thus, its replacement would be expected to have a deleterious effect on the mutant enzyme's structure and function. Modeling of the p.S47F/G111S mutant enzyme revealed that the two substitutions interacted to form a unique structure not present in the predicted structures for either single mutation (Figure 2). This interaction presumably resulted in the markedly reduced specific activity of the doubly mutant enzyme compared with either single mutant enzyme. Furthermore, the calculated total GROMOS energy (36) (and therefore predicted stability) for the p.S47F/G111S mutant was the lowest of all four predicted enzyme structures, consistent with the purified doubly mutant enzyme's reduced yield. Thus, the two amino acid substitutions in the enzyme acted synergistically to inactivate and destabilize the doubly mutant monomeric enzyme.

Neither the p.S47F nor p.G111S mutations have been reported in humans with CEP. Interestingly, a different mutation in codon 47 (c.139T>C, p.S47P) was reported in a CEP family in which several homozygous siblings had severe manifestations (37), consistent with its *in vitro* expression of <3% of expressed wild-type activity *in vitro* and <0.3% of wild-type activity in patient erythrocytes. In contrast to the phenylalanine substitution in the CEP cat, the proline substitution in human CEP (a residue known to

significantly alter protein structure) markedly decreased the human enzyme's function.

In summary, the cat described here is the first biochemically and genetically proven feline model of human CEP. The disease resulted from the interaction of two novel homozygous missense mutations that interacted to alter the enzyme's activity and stability. It should now be recognized that cats presenting with brownish discolored teeth may have either AIP or CEP. Differential diagnosis requires the quantitation of the porphyrin precursors and porphyrin isomers, determination of the URO-synthase or HMB-synthase enzyme activities or mutation analyses of the gene sequences. Future identification of cats with a CEP-like phenotype may detect additional cats with CEP, permitting the establishment of a colony and the opportunity to further investigate the disease pathogenesis and evaluate stem cell and gene transfer therapies prior to human trials.

DISCLOSURE

The authors declare that they have no competing interests as defined by *Molecular Medicine*, or other interests that might be perceived to influence the results and discussion reported in this paper.

REFERENCES

1. Clavero S, *et al.* (2010) Feline acute intermittent porphyria: a phenocopy masquerading as an erythropoietic porphyria due to dominant and recessive hydroxymethylbilane synthase mutations. *Hum. Mol. Genet.* 19:584–96.
2. Anderson KE, Sassa S, Bishop DF, Desnick RJ.

(2001) Disorders of heme biosynthesis: x-linked sideroblastic anemia and the porphyrias. In: *The Metabolic and Molecular Bases of Inherited Disease*. Scriver CS, Beaudet AL, Sly WS, Valle D (eds.). McGraw-Hill, New York, pp. 2991–3062.

3. Desnick RJ, Astrin KH. (2002) Congenital erythropoietic porphyria: advances in pathogenesis and treatment. *Br. J. Haematol*. 117:779–95.

4. Desnick RJ, Glass IA, Xu W, Solis C, Astrin KH. (1998) Molecular genetics of congenital erythropoietic porphyria. *Semin. Liver. Dis*. 18:77–84.

5. Shady AA, *et al*. (2002) Congenital erythropoietic porphyria: identification and expression of eight novel mutations in the uroporphyrinogen III synthase gene. *Br. J. Haematol*. 117:980–7.

6. Xu W, Warner CA, Desnick RJ. (1995) Congenital erythropoietic porphyria: identification and expression of 10 mutations in the uroporphyrinogen III synthase gene. *J. Clin. Invest*. 95:905–12.

7. Kauffman L, Evans DI, Stevens RF, Weinkove C. (1991) Bone-marrow transplantation for congenital erythropoietic porphyria. *Lancet*. 337:1510–1.

8. Shaw PH, Mancini AJ, McConnell JP, Brown D, Kletzel M. (2001) Treatment of congenital erythropoietic porphyria in children by allogeneic stem cell transplantation: a case report and review of the literature. *Bone Marrow Transplant*. 27:101–5.

9. Tezcan I, *et al*. (1998) Congenital erythropoietic porphyria successfully treated by allogeneic bone marrow transplantation. *Blood*. 92:4053–8.

10. Harada FA, Shwayder TA, Desnick RJ, Lim HW. (2001) Treatment of severe congenital erythropoietic porphyria by bone marrow transplantation. *J. Am. Acad. Dermatol*. 45:279–82.

11. Geronimi F, *et al*. (2003) Lentivirus-mediated gene transfer of uroporphyrinogen III synthase fully corrects the porphyric phenotype in human cells. *J. Mol. Med*. 81:310–20.

12. Kauppinen R, *et al*. (1998) Congenital erythropoietic porphyria: prolonged high-level expression and correction of the heme biosynthetic defect by retroviral-mediated gene transfer into porphyric and erythroid cells. *Mol. Genet. Metab*. 65:10–7.

13. Robert-Richard E, *et al*. (2008) Effective gene therapy of mice with congenital erythropoietic porphyria is facilitated by a survival advantage of corrected erythroid cells. *Am. J. Hum. Genet*. 82:113–24.

14. Aizencang G, Solis C, Bishop DF, Warner C, Desnick RJ. (2000) Human uroporphyrinogen-III synthase: genomic organization, alternative promoters, and erythroid-specific expression. *Genomics*. 70:223–31.

15. Aizencang GI, Bishop DF, Forrest D, Astrin KH, Desnick RJ. (2000) Uroporphyrinogen III synthase: an alternative promoter controls erythroid-specific expression in the murine gene. *J. Biol. Chem*. 275:2295–304.

16. Cunha L, *et al*. (2008) Human uroporphyrinogen III synthase: NMR-based mapping of the active site. *Proteins*. 71:855–73.

17. Fortian A, *et al*. (2009) Uroporphyrinogen III synthase mutations related to congenital erythropoietic porphyria identify a key helix for protein stability. *Biochemistry*. 48:454–61.

18. Mathews MA, *et al*. (2001) Crystal structure of human uroporphyrinogen III synthase. *EMBO J*. 20:5832–9.

19. Pontius JU, *et al*. (2007) Initial sequence and comparative analysis of the cat genome. *Genome Res*. 17:1675–89.

20. Chu TC, Chu EJ. (1962) Porphyrins from congenitally porphyric (pink-tooth) cattle. *Biochem. J*. 83:318–25.

21. Jørgensen SK, With TK. (1963) Porphyria in domestic animals: Danish observations in pigs and cattle and comparison with human porphyria. *Ann. N.Y. Acad. Sci*. 104:701–9.

22. Ichijo S, Konishi T, Sasaki S, Oboshi K. (1980) A case of bovine congenital porphyria (porphyria erythropoietica). *Nippon Juigaku Zasshi*. 42:725–9.

23. Yamashita C, *et al*. (1980) Congenital porphyria in swine. *Nippon Juigaku Zasshi*. 42:353–9.

24. Glenn BL. (1970) Feline porphyria: comparative aspects with porphyria of other animals and man. *Animal Models in Biomedical Research III*. Washington DC: National Academy of Sciences, pp. 135–48.

25. Giddens WE, Jr., Labbe RF, Swango LJ, Padgett GA. (1975) Feline congenital erythropoietic porphyria associated with severe anemia and renal disease: clinical, morphologic, and biochemical studies. *Am. J. Pathol*. 80:367–86.

26. Anderson PM, Desnick RJ. (1980) Purification and properties of uroporphyrinogen I synthase from human erythrocytes: identification of stable enzyme-substrate intermediates. *J. Biol. Chem*. 255:1993–9.

27. Tsai SF, Bishop DF, Desnick RJ. (1987) Coupled-enzyme and direct assays for uroporphyrinogen III synthase activity in human erythrocytes and cultured lymphoblasts: enzymatic diagnosis of heterozygotes and homozygotes with congenital erythropoietic porphyria. *Anal. Biochem*. 166:120–33.

28. Kiefer F, Arnold K, Kunzli M, Bordoli L, Schwede T. (2009) The SWISS-MODEL repository and associated resources. *Nucleic Acids Res*. 37: D387–92.

29. Schubert HL, Phillips JD, Heroux A, Hill CP. (2008) Structure and mechanistic implications of a uroporphyrinogen III synthase-product complex. *Biochemistry* 47:8648–55.

30. Glenn BL, Glenn HG, Omtvedt IT. (1968) Congenital porphyria in the domestic cat (Felis catus): preliminary investigations on inheritance pattern. *Am. J. Vet. Res*. 29:1653–7.

31. Tobias G. (1964) Congenital porphyria in a cat. *J. Am. Vet. Med. Assoc*. 145:462–3.

32. Jørgensen SK, With TK. (1955) Congenital porphyria in swine and cattle in Denmark. *Nature*. 176:156–8.

33. Clare NTS, Stephens EH. (1944) Congenital porphyria in pigs. *Nature*. 153:252–3.

34. Haydon M. (1975) Inherited congenital porphyria in calves. *Can. Vet. J*. 16:118–20.

35. Cooper DN, Youssoufian H. (1988) The CpG dinucleotide and human genetic disease. *Hum. Genet*. 78:151–5.

36. van Gunsteren WF, *et al*. (1996) *Biomolecular Simulation: The GROMOS 96 Manual and User Guide*.

Zürich: Swiss Federal Institute of Technology and the ETH, pp. 1044.

37. Ged C, *et al*. (2004) Congenital erythropoietic porphyria: report of a novel mutation with absence of clinical manifestations in a homozygous mutant sibling. *J. Invest. Dermatol*. 123:589–91.